Multidiszciplináris Tudományok, 14. kötet, 3. szám (2024) pp. 202-210. **https://doi.org/10.35925/j.multi.2024.3.18**

THE EFFECT OF RSW TECHNOLOGICAL PARAMETERS TO THE PROPERTIES OF ALUMINIUM/STEEL HYBRID JOINTS

Mariann Fodorné Cserépi
assistant lecturer, University of Miskolc, Institute of Materials Science and Technology
3515 Miskolc, Miskolc-Egyetemváros, e-mail: mariann.cserepi@uni-miskolc.hu

Ákos Meilinger
associate professor, University of Miskolc, Institute of Materials Science and Technology
3515 Miskolc, Miskolc-Egyetemváros, e-mail: akos.meilinger@uni-miskolc.hu

Abstract

To reduce fuel consumption and costs, the lightweight construction of car bodies is a very important aspect. This is achieved by using high-strength steel and aluminium alloy base materials. The latest car bodies contain both steel and aluminium alloy, so it is necessary to develop a reliable joining technology between them. Several joining technologies were investigated, such as mechanical joining, adhesive joining, and welding too. Resistance spot welding (RSW) is typically used to join car body parts and can be used for aluminium/steel hybrid joints. During welding, a very brittle intermetallic compound (IMC) is formed, which basically determines the properties of the joint, which is particularly influenced by the thickness and phases of the IMC. EN AW 5754 H22/ DP600 dissimilar joints were made with RSW, using different welding parameters. The joints were tested by shear-tensile tests and the effect of the IMC layer was determined.

Keywords: *hybrid joint, aluminium/steel joining, resistance spot welding (RSW), IMC*

1. Introduction

Nowadays, the aluminium/steel joining typically occurs in the automotive industry for car bodies, for example, energy-absorbing elements are often made of hybrid aluminium/steel structures. The structural elements should be joined together, and these joints can be made using mechanical connection methods or welding. In the case of self-piercing riveting, static tests such as tensile-shear or cross-tension tests show good joint strength (Karathanasopoulos and Mohr, 2022; Sakiyama et al., 2013), but rivets must be used for this process, which makes it more expensive. The clinching process is not expensive because it does not require the use of any additional material, but the joint strength is typically poor. In some cases, mechanical joining methods are complemented by adhesive bonding (Guzanová et al., 2023). Mechanical joining with adhesive bonding is a relatively expensive technology, welded joints can be more cost-effective. For welding, basically resistance spot welding (RSW) and ultrasonic welding (UW) can be used for spot joining with this material combination (Haddadi, 2016; Zhao et al., 2017; Patel et al., 2014).

Some studies (Sakiyama et al., 2013; Gullino, 2019) have highlighted that RSW is only rarely used for aluminium/steel sheet connections, because of the presence of brittle intermetallic compound (IMC), it is necessary to remove the oxide layer from the aluminium part before welding. In addition, the welding task is a challenge due to the completely different material properties (melting point, thermal

conductivity, electrical resistance, strength properties). The strength of the joint may be better with the oxide layer removed, but this process during production cannot be efficient and cheap enough, so in this study the welded joints were made without oxide removing. The second problem with welding is the presence of IMC because it has very brittle properties. The properties of the joint are influenced by the thickness of the IMC and the type of phase formed. (Meco et al., 2015) reported that a thin IMC layer thinner than 10 μm has no significant effect on the strength and ductility of joints, but a thick IMC layer may be detrimental, but in this case laser welding was used for the joint. In the case of RSW, researchers have come to different values for the optimal thickness of the IMC at the joint interface. In case of necessary to keep the temperature and duration of the process as low and as short as possible, since the formation of IMC requires atomic diffusion. In the case of IMC phases, there is a lot of research to identify the major phases and their effect on joining properties. Based on these, the joint properties may be better if the formation of Al-rich brittle IMC is minimized. The morphology and thickness of the IMC layer depends on the process parameters and the distance from the center of the joint; the thickness is generally greater at the joint center and lower at the edge (Zixuan et al., 2017). In the following paper, those welding parameter combinations can be found that are among which the IMC layer can be considered good. The mechanical properties of the test give acceptable results in the case of shear-tensile tests.

2. Materials

Materials often used in the automotive industry were chosen for the experiments. The steel side was DP600 combined with EN AW 5754 H22 aluminium alloy. Each base material was 1 mm thick for better comparability.

Aluminium sheet EN AW 5754 H22 is one of the most commonly used material grades, mainly due to its good formability and also good strength properties. The main alloying element is Mg, its strength was increased by forming, and then it is softened to a quarter of hardness. Table 1. shows the chemical composition of aluminium alloy according to the material certificate.

Table 1. *Chemical compositions of the applied aluminium alloy, weight %*

Base material	Cu	Fe	Mn	Cr	Mg	Ti	Si	Zn	Al
EN AW 5754 H22	0.055	0.294	0.358	0.009	2.796	0.016	0.193	0.034	rest

DP600 steel was chosen as the steel component, it has a relatively low strength among the dual phase (DP) steels. DP steels contain martensite islands embedded in a ferrite matrix with a dispersed distribution. Table 2. shows the chemical composition of DP600 steel according to the material certificate.

Table 2. *Chemical composition of the applied DP steel, weight %*

Base material	C	Si	Mn	P	S	Nb	V	B	Fe
DP600	0.098	0.2	0.81	0.015	0.002	0.014	0.010	0.0002	rest

Table 3. shows the main mechanical properties of the base materials according to quality certificates (tensile strength (R_m), yield strength ($R_{p0.2}$) and elongation (A_{50}).

Table 3. *Basic mechanical properties of base materials*

Base material	R_m [MPa]	$R_{p0,2}$ [MPa]	A_{50} [%]
EN AW 5754 H22	220	137	22
DP600	669	448	18.7

3. Welding and testing circumstances

A TECNA 8007 type resistance spot welding equipment (AC, 50 Hz) with a TE 550 type control was used for joining. The welding force was provided by a pneumatic cylinder.

Figure 1. *TECNA 8007 type resistance spot welding equipment*

The material of the electrode used was class 2 (CuCrZr) according to RWMA. The welding electrodes have a tip head diameter of 5 mm, which must be chosen depending on the thickness of the sheet to be welded. For a sheet thickness of 1 mm, we used a radius of R=50 mm as recommended in the literature (Eldos, 2019; Gáspár et al., 2020) The same geometry was used for the top and bottom electrodes. (Figure 2.)

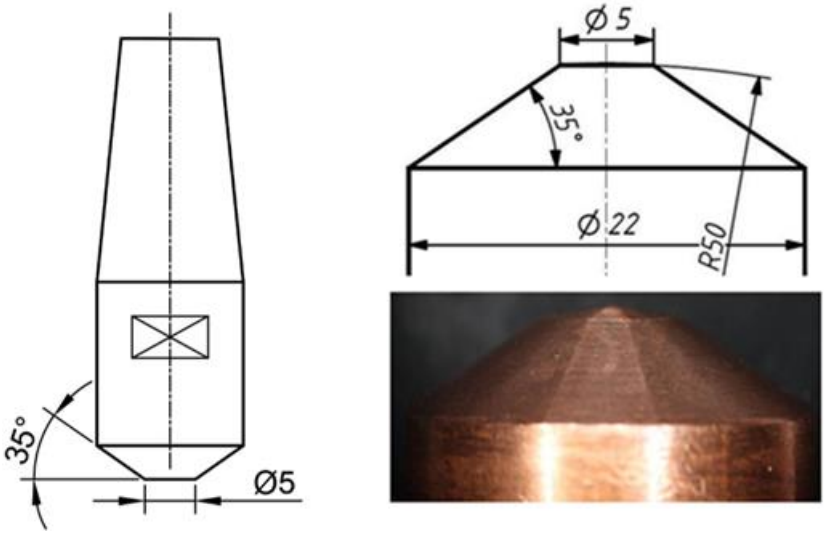

Figure 2. *The geometry of the electrode used for welding*

One of the most important tests for determining the mechanical properties of resistance spot-welded joints is the tensile-shear test. The reason for this is, among other things, the simple geometry of the tested specimen and the simplicity of the test.

The effect of welding parameters can be influential for the intermetallic compound (IMC) thickness, which is formed in the joint interface. In this research, we focus on the effect of welding current and welding time with same welding force. Table 4. shows the parameter combinations which are investigated.

Table 4. *Applied welding parameters*

Number	**Current I_h[kA]**	**Welding time t_h[per]**	**Electrode force F_e[kN]**
1	14	6	2.5
2	16	6	2.5
3	14	10	2.5
4	16	10	2.5
5	14	12	2.5
6	16	12	2.5
7	14	14	2.5
8	16	14	2.5
9	14	16	2.5
10	16	16	2.5
11	14	18	2.5
12	16	18	2.5
13	14	20	2.5
14	16	20	2.5

The welding parameters were determined according to previous investigations.

4-4 samples were welded from every parameter combination. 3 samples were tensile-shear tested, 1 sample was used for intermetallic compound (IMC) layer measuring.

For IMC thickness measuring the joint was cut in the middle and fixed in epoxy. Then grinded with P120 – P1500 grinding papers, after polishing happens. Nital (3% HNO_3 + 97% etanol) was used for etching (15 sec). The etched surface was checked by optical microscope.

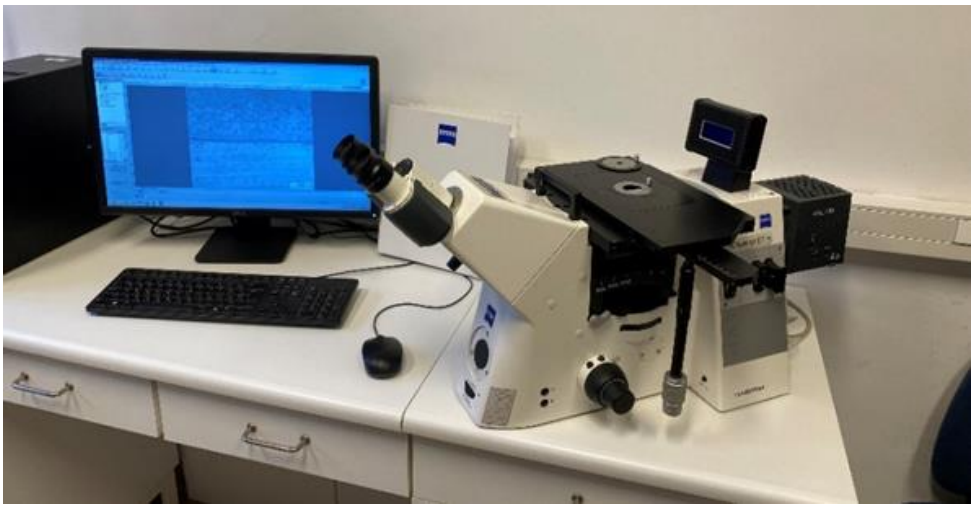

Figure 3. *Zeiss Observer D1.M type optical microscope for IMC thickness measuring*

1000x magnification was necessary to use.

The tensile-shear (TS) test specimens were tested with an MTS-type electrohydraulic universal material testing equipment, which is illustrated in Figure 4.

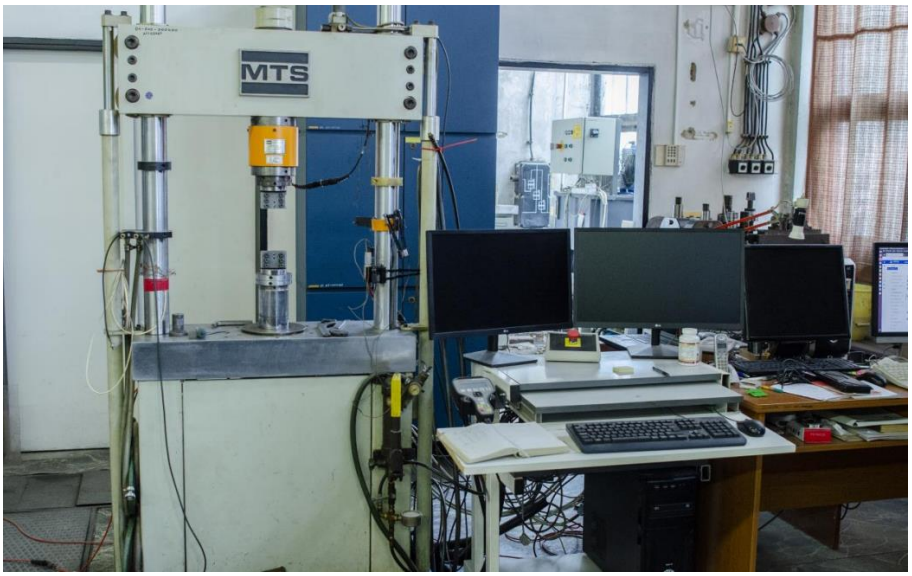

Figure 4. *MTS electrohydraulic tensile machine*

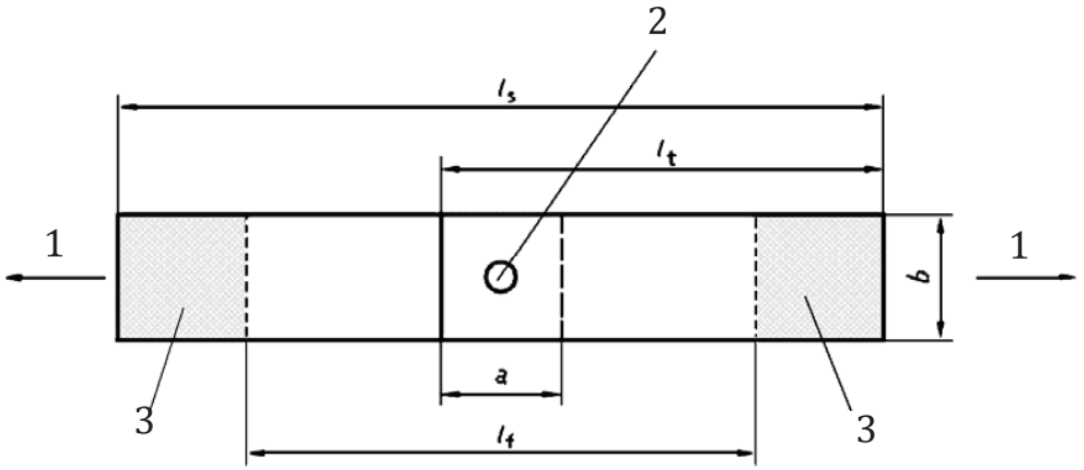

Figure 5. *Geometric dimensions of the specimen used during the tensile shear test. (1: load direction, 2: scar lens, 3: capture area)*

The test specimens were designed according to Figure 5.

The base material was cut into 100 mm × 30 mm dimensions. The RSW connection area is located in the center with an overlap of 30 mm. The principle of the test is that the overlapped joints are clamped in a clamping tool and pull at a uniform speed (in this case the speed was 0,2 mm/s). During the test, the joint is loaded to failure. This can be of three types:

- the spot is plugging out from the sheet (plug failure),
- the spot is partially plugging out from the sheet (partial plug failure),
- shearing happen in the joint interface (interfacial failure).

During the test, the maximum tensile strength, the tensile diagram and failure mode are recorded.

4. Results and discussion

In this section, the results of IMC measuring and tensile-shear tests are compared. Table x. the average IMC thicknesses (h_{IMC}) and their deviation ($h_{IMC\ dev}$), the average tensile-shear forces (F_{TS}) and their deviation ($F_{TS\ dev}$). According to previous investigations, joint thickness can be also important, so it was measured and written in this table. The failure mode was also observed, this is the last column of this table.

According to Table 5. the joint thicknesses are lower in case of 16 kA and longer welding time. The average IMC thicknesses change between 1,162 and 2,194 μm. Thicker IMC layers are measured in case of longer welding times. The standard deviation of IMC thickness is lower in case of thinner layers and higher in case of thicker IMC layers. The average tensile-shear forces are between 1,443 kN and 3,14 kN, which is a significant difference. The standard deviation of tensile-shear force is an important result, it shows the repeatability of the technology. In this case the joints that are made with longer welding time shows better repeatability. In case of the highest tensile-shear forces, the failure mode was plug, interfacial failure mode resulted lower tensile-shear force.

Figure 6. shows the average IMC thicknesses and average tensile-shear forces as a function of welding time in case of 14 kA welding current.

Table 5. *Results of tests (h = joint thickness, h_{IMC} = IMC thickness, $h_{IMC\ dev}$ = standard deviation of IMC thickness, F_{TS} = tensile-shear force, $F_{TS\ dev}$ = standard deviation of tensile-shear force)*

No.	h [mm]	$\bar{h}_{IMC}$ [µm]	$h_{IMC\ dev}$ [µm]	$\bar{F}_{ts}$ [kN]	$F_{ts\ dev}$ [kN]	Failure mode
1	1,6	1,162	0,167	2,056	0,286	interfacial
2	1,52	1,371	0,167	2,476	0,510	interfacial
3	1,5	1,354	0,201	2,346	0,923	interfacial
4	1,45	1,403	0,163	2,813	0,329	plug
5	1,5	1,470	0,190	1,923	1,109	interfacial
6	1,35	1,341	0,176	1,443	0,455	interfacial
7	1,55	1,539	0,265	2,740	0,303	interfacial
8	1,45	1,930	0,400	2,766	0,234	interfacial
9	1,53	1,552	0,312	1,893	1,234	interfacial
10	1,38	2,002	0,305	1,643	0,855	interfacial
11	1,52	1,632	0,274	2,936	0,335	interfacial
12	1,37	1,794	0,377	3,110	0,125	plug
13	1,47	2,194	0,424	2,720	0,134	interfacial
14	1,35	1,863	0,284	3,140	0,202	plug

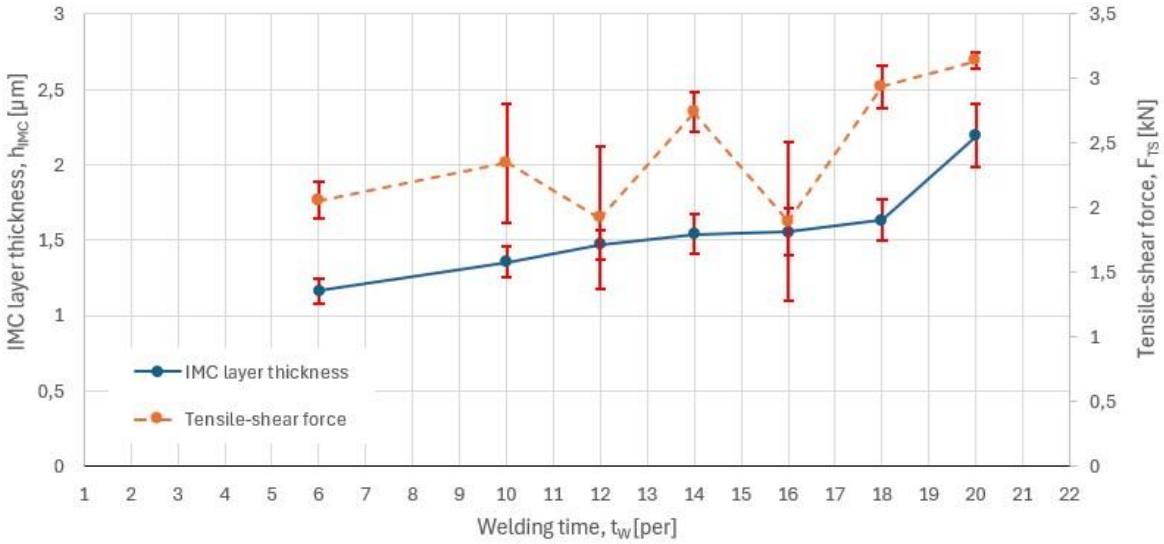

Figure 6. *IMC thickness and tensile-shear force results in case of 14 kA*

The IMC thickness is continuously growing with longer welding times. The tensile-shear forces are increasing by increasing welding time, except in case of 12 and 16 periods. The highest tensile-shear forces were reached by the longest welding time. The standard deviation of tensile-shear strength in case of 12 and 16 periods are huge, which means that the repeatability is poor in these cases.

Figure 7. shows the average IMC thicknesses and average tensile-shear forces as a function of welding time in case of 16 kA welding current.

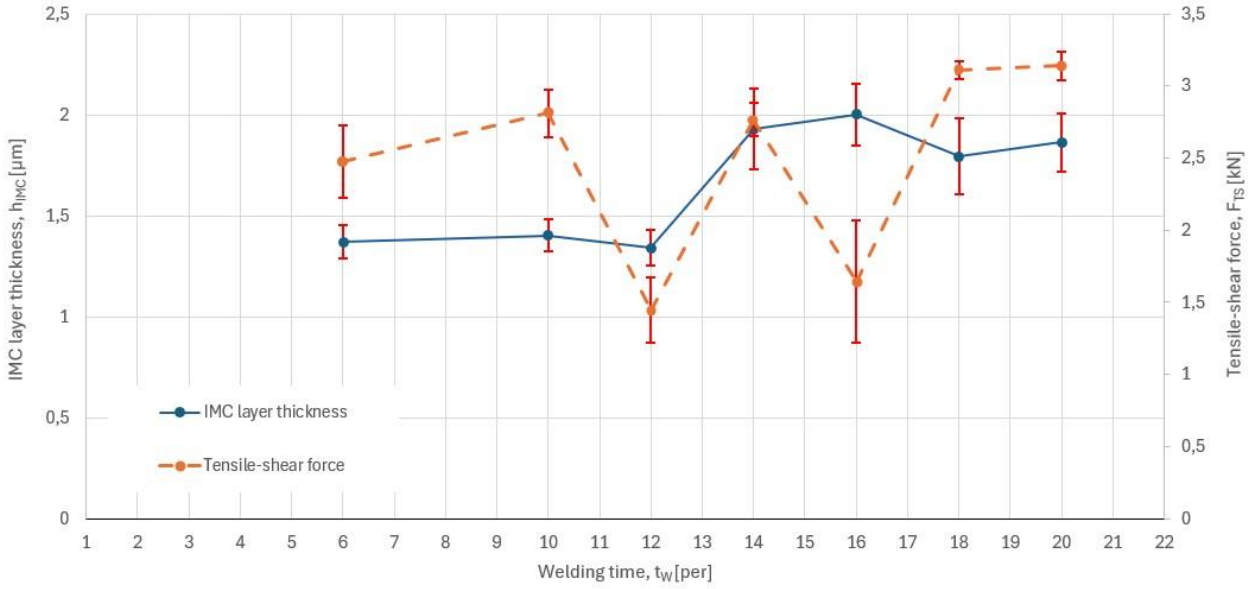

Figure 7. *IMC thickness and tensile-shear force results in case of 16 kA*

In this figure the IMC thickness is growing with the welding time but not as linearly as in the previous case. After 16 periods (320 ms) the IMC thickness is not changing significantly. Interestingly the tensile-shear forces increase with the welding time except in case of 12 and 16 periods, like in case of 14 kA. The standard deviations are huge too in these cases. The best results come from the longer weld time as in the previous case.

5. Conclusions

According to the result of the investigation, the following conclusions can be drawn:

- In case of 1mm thick 5754-H22/DP600 hybrid joint, different welding parameters have effect to the IMC thickness and joint thickness, too.
- Longer welding time significantly causes a thicker IMC layer, but with the lower welding current (14 kA) the IMC thickness grows almost linearly, while with higher welding current (16 kA) it grows till 16 periods and then remains the same thickness.
- The longer welding time causes thicker IMC layers and better tensile-shear forces in all cases.
- The bigger tensile-shear forces resulted plug failure mode.
- In case of 12 and 16 periods the tensile-shear forces are dropped, the repeatability of these joints is poor. Additional investigation is needed to find the reason.

References

[1] Karathanasopoulos, N., Mohr, D. (2022). Strength and failure of self-piercing riveted aluminum and steel sheet joints: Multi-axial experiments and modeling. *Journal of Advanced Joining Processes, 5*, 100107, 1–9. **https://doi.org/10.1016/j.jajp.2022.100107**

[2] Sakiyama, T., Gen Murayama, G., Yasuaki Naito Y., Kenji Saita, K., Miyazaki, Y., Oikawa, H., Nose, T. (2013). *Dissimilar metal joining technologies for steel sheet and aluminum alloy sheet in auto body*. Nippon Steel Technical Report No. 103, 91–97. https://www.nipponsteel.com/en/tech/report/nsc/pdf/103-14.pdf

[3] Guzanová, A., Brezinová, J., Varga, J., Džupon, M., Vojtko, M., Janoško, E., Viňáš, J., Draganovská, D., Hašul, J. (2023). Experimental study of steel–aluminum joints made by RSW with insert element and adhesive bonding. *Materials, 16*, 864. **https://doi.org/10.3390/ma16020864**

[4] Haddadi, F. (2016). Microstructure reaction control of dissimilar automotive aluminium to galvanized steel sheets ultrasonic spot welding. *Materials Science & Engineering A 2016, 678*, 72–84. **https://doi.org/10.1016/j.msea.2016.09.093**

[5] Zhao, D., Ren, D., Zhao, K., Pan, S., Guo, X. (2017). Effect of welding parameters on tensile strength of ultrasonic spot welded joints of aluminum to steel—By experimentation and artificial neural network. *Journal of Manufacturing Processes, 30*, 63–74. **https://doi.org/10.1016/j.jmapro.2017.08.009**

[6] Patel, V. K., Bhole, S. D., Chen, D. L. (2014). Ultrasonic spot welding of aluminum to high-strength low-alloy steel: Microstructure, tensile and fatigue properties. *Metallurgical and Materials Transactions A 2014, 45*, 2055–2066. **https://doi.org/10.1007/s11661-013-2123-y**

[7] Gullino, A. (2019). Review of aluminum-to-steel welding technologies for car-body applications. *Metals, 9*, 315. **https://doi.org/10.3390/met9030315**

[8] Meco, S., Pardal, G., Ganguly, S., Williams, S., McPherson, N. (2015). Application of laser in seam welding of dissimilar steel to aluminium joints for thick structural components. *Optics and Lasers in Engineering, 67*, 22–30. **https://doi.org/10.1016/j.optlaseng.2014.10.006**

[9] Zixuan, W., Hui-Ping, W., Nannan, C., Min, W., Blair, E. C. (2017). Characterization of intermetallic compound at the interfaces of Al-steel resistance spot welds. *Journal of Materials Processing Technology, 242*, 12–23. **https://doi.org/10.1016/j.jmatprotec.2016.11.017**

[10] Eldos, Z. A. (2019). Prediction and stabilization of initial resistance between electrodes for small-scale resistance spot welding. *Welding in the World, 63*, 443–457. **https://doi.org/10.1007/s40194-018-0671-x**

[11] Gáspár, M., Dobosy, Á., Tisza, M., Török, I., Yangchun, D., Kailun, Z. (2020). Improving the properties of AA7075 resistance spot-welded joints by chemical oxide removal and post weld heat treating. *Welding in the World, 64*, 2119–2128. **https://doi.org/10.1007/s40194-020-00988-y**